Green Chemistry

PAPER

View Article Online
View Journal | View Issue

Cite this: *Green Chem.*, 2024, **26**, 8298

Low-chromophore lignin isolation from natural biomass with polyol-based deep eutectic solvents†

Jinyuan Cheng, [a,b] Xuelian Zhou,[a] Caoxing Huang,[b] Chang Geun Yoo, [f] Xianzhi Meng, [c] Guigan Fang,*[a,b] Arthur J. Ragauskas [c,d,e] and Chen Huang*[a,b]

Received 14th April 2024,
Accepted 7th June 2024

DOI: 10.1039/d4gc01824a

rsc.li/greenchem

When attempting to obtain light-color lignin from lignocellulosic biomass or industrial lignin, the available options based on chemical or morphological modification suffer from low yield, high cost, and lack of availability at the required scales. In this study, we adopted a polyhydric-alcohol-based deep eutectic solvent (PA-DES) to directly extract light-color lignin from natural biomass, which is even whiter than native cellulolytic enzyme lignin (CEL). The isolated lignin possessed a high recovery yield (97.36%), regular micro-spherical morphology, enriched β-ether linkage of 58/100Ar, low phenolic hydroxyl content of 1.25 mmol g^{-1}, minimal carbonyl content of 0.70 mmol g^{-1}, and less condensed structures, thus yielding a lower content of chromophores. This lignin showed excellent sunscreen effects, which could enhance the SPF of a commercial sunscreen from 15 to 40 with only 5 wt% addition. This study can provide essential guidance for the scale-up production of light-color lignin and obtaining near-complete digestible cellulose for further saccharification.

1. Introduction

In the context of carbon neutrality, there is an urgent need to explore and develop renewable and sustainable resources to reduce the growing energy consumption and environmental problems caused by over-reliance on fossil fuels.[1] Lignocellulose, which consists of cellulose (30–50%), hemicellulose (10–35%), and lignin (15–35%), is the most abundant and sustainable green carbon resource on Earth.[2] Utilization of lignocellulosic biomass is a feasible approach for achieving carbon neutrality. However, the natural recalcitrant structure and stubborn lignin-carbohydrate complex (LCC) frameworks make it difficult to valorize lignocellulose.[3] Thus, fractionation of biomass becomes an essential prerequisite for obtaining high value-added chemicals and products. Conventionally, carbohydrate-centered processes focusing on (hemi) cellulose utilization are the mainstream, including dilute sulfuric acid treatment, kraft cooking, or sulfite processes, while in these methods, lignin is irreversibly degraded or converted to a condensed product with dark color, which makes it difficult to be utilized.[4] Recently, methods such as organic acid[5] and organosolv fractionation[6] have been widely investigated for the pretreatment of biomass and isolation of lignin for value-added upgrading. Although these fractionation strategies can extract lignin with a relative high reactivity, the recovered lignin still features a dark color.[7] The undesired dark color of isolated lignin greatly constrains its high-value applications, such as dye disperser and sunscreen additives. Therefore, it is important to whiten lignin, especially during its isolation process, to an acceptable color to expand its valorization.

Bamboo is a perennial gramineous plant which is widely distributed in China. There are 300 species belonging to 44 genera which are native to China, covering a bamboo forest of ~76 000 km^2 and accounting for 3.3% of total forest area.[8] Bamboo shoots after a spring rain can grow over 100 cm day^{-1},[9] which could be harvested in 1–5 years. Similar in composition to hardwood, bamboo is mainly composed of cellulose (30%–50%), hemicellulose (10%–30%) and lignin (15%–35%).[10] Cellulose (glucan) in bamboo is a linear bio-macromolecule connected by 1,4-β-glucosidic bonds, while hemicellulose is a heterosaccharide including main xylan and minor araban with branched chains.[11] The lignin in bamboo is primarily made up of three phenylpropane monomers,

[a]*Institute of Chemical Industry of Forest Products, Chinese Academy of Forestry, Jiangsu Province Key Laboratory of Biomass Energy and Materials, Nanjing 210042, China. E-mail: huangchen3127@njfu.edu.cn*
[b]*Co-Innovation Center for Efficient Processing and Utilization of Forest Resources, Nanjing Forestry University, Nanjing 210037, China. E-mail: fangguigan@icifp.cn*
[c]*Department of Chemical and Biomolecular Engineering, University of Tennessee Knoxville, Knoxville, TN 37996, USA. E-mail: aragausk@utk.edu*
[d]*Department of Forestry, Wildlife, and Fisheries, Center for Renewable Carbon, The University of Tennessee Institute of Agriculture, Knoxville, TN 37996, USA*
[e]*Joint Institute for Biological Science, Biosciences Division, Oak Ridge National Laboratory, Oak Ridge, TN 37831, USA*
[f]*Department of Paper and Bioprocess Engineering, State University of New York College of Environmental Science and Forestry, Syracuse, New York 13210-2781, USA*
†Electronic supplementary information (ESI) available. See DOI: https://doi.org/10.1039/d4gc01824a

including guaiacyl (30%–50%), syringyl (50%–70%) and *p*-hydroxyphenyl (5%–15%), which are mutually cross-linked *via* C–O–C (50%–70%) and C–C (10%–20%) bonds.[12] The S/G ratio of bamboo is ~2 : 1, meaning that the methoxy group is abundant in bamboo lignin. One research hotspot is for fermentable sugar production usually by sequential pretreatment and enzymatic saccharification.[13] The pretreatment methods include hydrothermal,[14] diluted alkaline,[15] organic solvent,[16] ionic liquid and/or combined pretreatments.[17] Although these pretreatment methods could well convert carbohydrates into its corresponding mono sugars, the lignin utilization of bamboo is still in its infancy. Therefore, it is of great sense for establishing a sustainable method for realizing lignin valorization.

Deep eutectic solvents (DES) consist of one hydrogen bond acceptor (HBA), usually a quaternary ammonium cation with a halide anion (*e.g.*, benzyltrimethylammonium chloride (BTEAC) and choline chloride), and at least one hydrogen bond donor (HBD) such as organic acids and polyhydric alcohols, which possess a lower melting point than that of each constituent.[18] ChCl and BTEAC are the most commonly used HBAs, and both of them have a similar performance, price and recyclability, but BTEAC has poor thermal stability and high toxicity.[19] Therefore, ChCl is the better HBA due to its good thermal stability and very low toxicity, and it is also added as a vitamin to chicken feeds. Compared with ionic liquids, the DES have outstanding properties such as environmental friendliness, low cost, biodegradability, and non-flammability and show excellent dissociation of lignin and hemicellulose while preserving cellulose during lignocellulose fractionation.[20,21] However, previous DES fractionation processes paid too much attention to the isolation of lignin and hemicellulose to enhance cellulose accessibility, while neglecting the lignin quality and its upgrading potential, with a common dark color issue. For example, Shen *et al.* established a ChCl/lactic acid system for Eucalyptus fractionation, which obtained a 94.3% glucan saccharification yield, while the recovered lignin was greatly depolymerized, accompanied by severe condensation reactions.[22] Another study using ChCl/*p*-hydroxybenzoic acid for poplar fractionation obtained a glucose yield of over 90%, but this process also faced severe degradation and condensation reactions for the recovered lignin.[23] Excessive degradation and condensation of the isolated lignin greatly reduce the reactivity of lignin and darken the color of lignin, which limit lignin valorization in dye disperser or sunscreen additives. The lignin degradation and condensation reactions were greatly determined by the HBD type. For example, organic acid HBDs such as lactic acid, oxalic acid and *p*-toluenesulfonic acid could provide protons to cleave the aryl-ether of the lignin and facilitate the condensation. Accompanied by these common organic acid HBDs, polyhydric alcohol (PA) HBDs have a little cleaving ability for the bonds of lignin while possessing an excellent solubility and protection ability for lignin, thus they could isolate lignin without scarifying its structure. However, the natural recalcitrance of lignin-carbohydrate compounds (LCC) of lignocellulose greatly constrains the lignin isolation when using the PA type as the HBD. To solve this, acidic chemicals such as sulfuric acid, oxalic acid and Lewis acids are good candidates for assisting the lignin isolation process by cleaving the LCC bonds. Herein, the principles for selecting the HBD should base on the lignin dissolving assisted by the LCC bond cleavage rather than the severe degradation of lignin.

Natural lignin is light brown and has a strong UV-shielding property, which is considered an ideal choice for sunscreen production.[24] However, during lignin isolation, especially under harsh conditions (*e.g.*, strong acidity, high temperature, and a long fractionation time), various chromophore groups induced by the formation of carbon–carbon double bonds conjugated with aromatic rings, quinone methides, quinones, chalcone structures, or metal complexes with catechol structures darken lignin.[16,25,26] The dark color of the lignin is one of the main obstacles for its application as a sunscreen. Numerous strategies have been proposed to decrease chromophore groups and whiten lignin by modifying its morphology and/or chemical structure. For example, ground lignin with tiny particles is obviously color-reduced by more than threefold compared with untreated lignin.[27] In addition, significant color fading of Kraft lignin was obtained through the rearrangement of chromophores by self-assembly into colloidal spheres.[16] In another study, acetylation treatment was used to protect the phenolic hydroxyl groups to change the color of alkaline lignin from black to brown.[26] In brief, previous processes to obtain light-color lignin mainly relied on the decoloration of commercial lignin by complicated processes with a very low yield (<10%), whereas the direct output of light-color lignin by the combination of morphology mediation and structural stabilization from lignocellulose biomass in one pot at the same time obtaining a digestible cellulose-rich solid has not yet been reported.

Recently, we found that polyol as the HBD in DESs for lignocellulose fractionation could protect lignin from further degradation and condensation. Thus, it is plausible that this method could reduce the color of the isolated lignin. In this study, light-color lignin was obtained by various PA-DES pretreatments of natural bamboo under mild conditions (110 °C for 1 h). This study unveiled the formation mechanism of light-color lignin through morphology regulation and chemical structure stabilization, which will provide promising guidance for methods and mechanisms to obtain high-yield and light-color lignin at the same time enhancing cellulose saccharification for the high-value upgrading of lignocellulose.

2. Results and discussion

2.1. DES viscosity and its KamLet-Taft empirical parameters

The viscosity representing the permeation and swelling effect of a DES is considered one of the essential parameters for the lignocellulose fractionation.[28] As shown in Table S1,† the viscosities of the different PA-DESs differed a lot at a lower temperature of 30 °C which were 110 (GLDES), 108 (BDDES) and

60 mPa s (EGDES), while all of them significantly decreased as the temperature increased, and finally reached a very similar value of ~7 mPa s. This result indicated that the viscosity of different DES systems at mild pretreatment temperatures might greatly determine the fractionation performance, while it possibly has a little influence in a severe pretreatment.

Generally, the fractionation ability of lignocellulose might have a relationship with the KamLet-Taft empirical parameters represented by α, β, and π^* parameters which quantified the hydrogen-bond donating ability (acidity), hydrogen-bond accepting ability (basicity), and dipolarity/polarizability of DESs, respectively.[29] In order to better understand the pretreatment efficiency of the prepared DESs, the KamLet-Taft empirical parameters, including α, β and π^*, were determined (Table S2†). After analyzing the data carefully, we found that the GLDES system possessed higher α–β and π^* values, indicating the higher hydrogen-bond donor ability and stronger dipolarity/polarizability, which might have a more efficient fractionation ability. However, the β values of the DESs were negative and have an opposite trend to the values of α–β and π^*, indicating that a lower β value might be favorable for the lignocellulose fractionation performance.

2.2. Selective degradation of lignin and hemicellulose

After pretreatment, ethanol solution was added to sufficiently separate and recover the cellulose and lignin. The cellulose-rich solids in the mixture were separated by filtration, and the lignin was recovered by evaporating the ethanol and adding the antisolvent of water, while xylan substantially degraded in the liquid which is hard to recover. The ChCl/glycerol/$AlCl_3$ (GLDES) system was first used to determine the optimal pretreatment conditions for PA-DES. As shown in Fig. 1A, the solid yield significantly decreased from 73.28% to 58.63% as the temperature increased from 100 °C to 110 °C, while it remained nearly constant as the temperature enhanced to 120 °C. For the variations of the major constituents in the pretreatment from 100 to 120 °C, xylan removal increased from 62.98% to 86.40%, and lignin removal also showed the same trend from 22.86% to 70.74%. In the case of glucan, its recovery remained constant (94.15%–95.32%) despite the increase in temperature, implying that glucan was very stable during GLDES treatment. Further increasing the temperature might result in the decrease of lignin removal (data are not shown) by generating unproductive lignin condensation and pseudo lignin which could cause damage to the quality of lignin and subsequent carbohydrates' saccharification process.[30] Considering the satisfactory removal of lignin (66.20%) and xylan (80.23%) and the near-complete preservation of glucan (95.32%) at 110 °C, this temperature was chosen for the investigation of other PA-DES pretreatments.

ChCl/ethylene glycol/$AlCl_3$ (EGDES) and ChCl/butanediol/$AlCl_3$ (BDDES) were studied using the same procedures and compared with GLDES. The composition analyses of the different PA-DES systems are shown in Fig. 1B. The solid yield of EGDES was 67.81% and that of BDDES was 59.29%, slightly higher than that of GLDES, but it still showed significant fractionation performance. Furthermore, xylan removal was 65.97–80.23% in different PA-DES treatment systems, in which EGDES showed the lowest xylan removal, while GLDES obtained the highest one. The excellent hemicellulose removal in GLDES might be ascribed to the stronger H-bond interaction, because GL with three OHs has a higher H-bond donating ability.[31] In addition, lignin removal also depended on the PA type, which increased from 55.07% (EGDES) to 66.20% (GLDES) but reached the highest value of 70.63% for BDDES. This trend indicates that the H-bond quantity alone cannot determine the pretreatment performance; other factors, such as the inherent solvent properties, also have a significant effect.

For cellulose, the glucan recovery yields could reach 95.32–99.04% throughout the different PA-DES systems, suggesting that all the PA-DES fractionations could preserve the cellulose. Benefitting from the degradation of hemicellulose/lignin, the pretreated solids exhibited excellent enzymatic saccharification yields (Fig. S1†). Raw bamboo had a limited saccharification yield, with only 12.63% glucan and 1.74% xylan saccharification yields (Fig. S1†). After EGDES pretreatment, the glucan and xylan saccharification yields dramatically increased to 86.82% and 95.78%, respectively, which were enhanced by 6.87 and 50.05 times compared to the raw bamboo, respectively. Both GLDES and BDDES led to over 90% of glucan and xylan saccharification yields, outperforming other conventional DESs such as ChCl/formic acid,[32] ChCl/oxalic acid,[33] and ChCl/*p*-hydroxybenzoic acid.[23] These results implied that our PA-DESs could easily achieve satisfactory carbohydrate conversion through enzymatic hydrolysis.

2.3. Lignin characterization

2.3.1. Lignin recovery, carbohydrate analysis and elemental quantification. After DES fractionation, lignin recovery yield and its components were determined (Table S3†). It can be seen that the isolated lignins of PA-DESs showed near-complete recoveries (94.62–97.36%), which are higher than most reported fractionation systems such as alkaline[34] and organosolv processes,[6,35] indicating that the proposed PA-DES fractionation system could easily regenerate lignin from lignocellulose. We also performed the pretreatments using traditional ChCl/lactic acid (LADES) and ChCl/oxalic acid (OADES); the lignin recovery yields in these methods were only 79.65% and 75.68%, respectively. This is likely because lignin in conventional acid DES pretreatment usually suffers from serious degradation and condensation that precipitate back onto the substrate surface. In contrast, PA-DES partially protected the lignin degradation products from being depolymerized and condensed, which resulted in an intact lignin structure, thus decreasing its loss during the anti-solvent precipitation process and facilitating its recovery.

Considering the high lignin recovery yields and significant xylan removal during the fractionation processes, polysaccharides may be present in the recovered lignin, which is detrimental to further valorization. Thus, component analysis was conducted to analyze its purity (Table S3†). Surprisingly, only trace

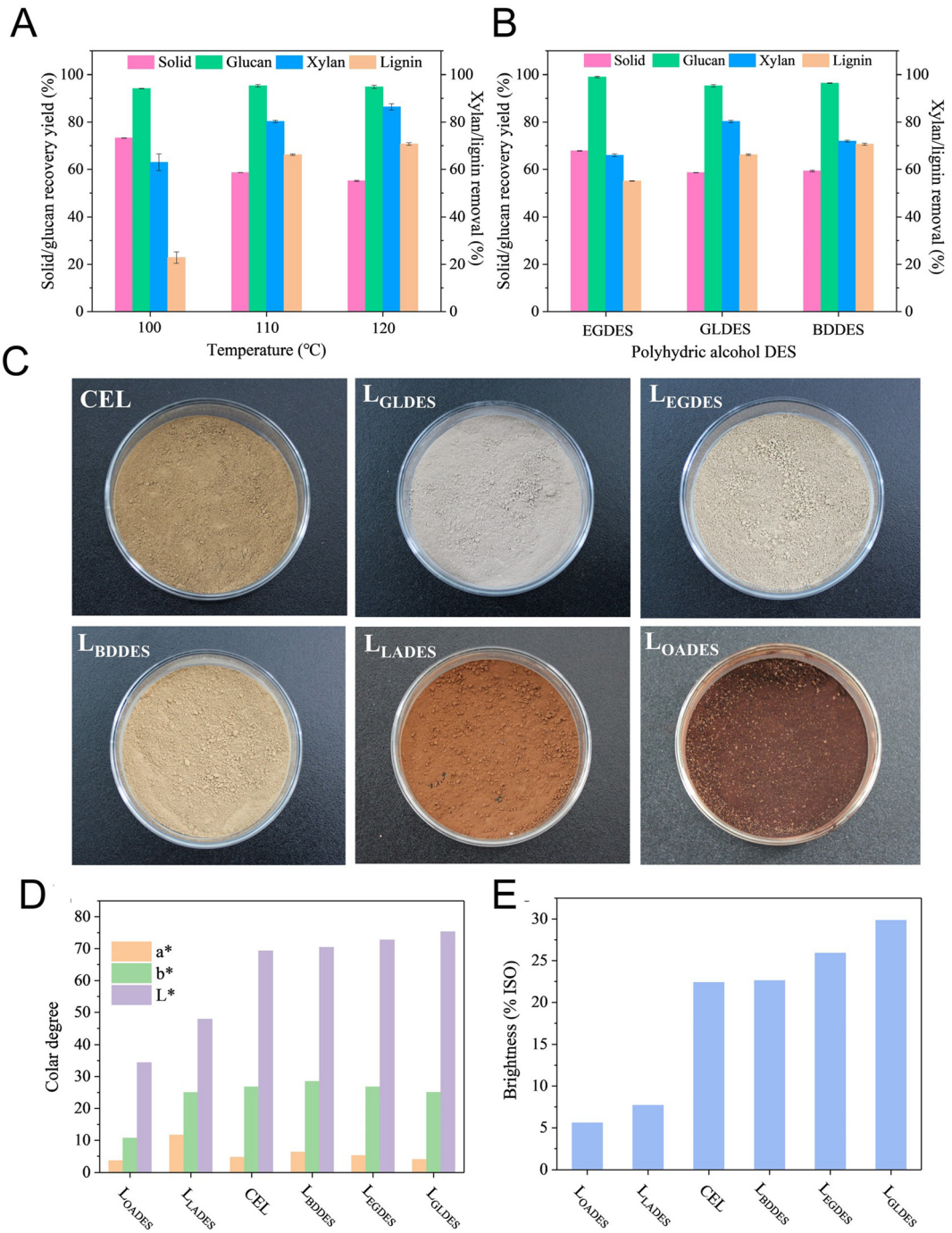

Fig. 1 Components of fractionated bamboo and lignin morphology analysis. (A) Component analysis after GLDES pretreatment at different temperatures and (B) different PA-DES systems at 110 °C; (C) digital photographs of the recovered lignins; (D) *L**, *a**, and *b** values of the recovered lignins, and (E) the brightness of the recovered lignins.

polysaccharides were tested in the regenerated lignin (less than 0.11% glucan and 0.16% xylan), implying the high purity of the recovered lignin. The high-purity lignins recovered from our PA-DESs were favorable for further valorization.

The difference in elemental composition of the lignin, extracted from bamboo using different DES systems, was not so distinct (Table S4†). For CEL, it contains 59.04% C, 5.69% H, 0.29% N. Compared with CEL, the lignin recovered from the organic acid-based DES of L_{LADES} and L_{OADES} possessed a higher C content, while the lignin isolated by PA-DES had a lower C content, especially L_{GLDES}. The content of C element in the L_{OADES} was the highest, 60.64%, followed by L_{LADES} (59.04%), and was the lowest in the L_{GLDES}. During the lignin isolation process, lignin condensation reactions result in more

C–C bonds which could lead to a higher content of C element. This assumption will be further discussed in the following 2D HSQC NMR quantification result. As for the H element, it is higher in the PA-DES induced lignin than the lignins extracted using organic acid-based DESs. In addition, the N element in the DES lignin was quite higher than the CEL, and this result could be ascribed to the ChCl residual in the isolated lignin.

2.3.2. Color appearance and morphological analysis. The appearance of the recovered lignins is shown in Fig. 1C; lignin extracted through the PA-DES systems exhibited a light brown color, which was even whiter than that of the native CEL. In contrast, lignin isolated from organic acid-based DESs (LADES and OADES) featured a dark brown color. The bulk density of the isolated lignins was macroscopically quantified. The lignins recovered from both the OADES and LADES systems have a high bulk density of 0.58 and 0.55 g cm^{-1}, respectively (Fig. S2†). However, the bulk density of lignins recovered from the PA-DES fractionation system ranged from 0.24 to 0.28 g cm^{-1}, over 50% lower than that of the OADES and LADES, indicating their bulk macrostructure. Specifically, the visible color of the recovered lignins was negatively correlated with their bulk density, suggesting that a higher bulk density might have a tight structure and result in a dark color.

To quantify the differences in the color of the recovered lignins, the lignin samples were further evaluated using $L^*a^*b^*$ values and brightness. As shown in Fig. 1D, the L^*, a^*, and b^* values in the native bamboo CEL were 69.32, 4.72, and 26.75, respectively. The lignins recovered from the PA-DESs had similar $L^*a^*b^*$ values, close to that of native CEL, which explained why our PA-DESs could yield light-color lignin. In contrast, lignins from both organic acid-based DESs had extraordinary lower $L^*a^*b^*$ values, especially L_{OADES}, which possessed $L^*a^*b^*$ values of 34.33, 3.61, and 10.71, respectively. For brightness, it is 22.39% ISO for native CEL. After traditional acidic OADES and LADES fractionation, lignin brightness decreased significantly to 5.59 and 7.69% ISO, respectively (Fig. 1E). Importantly, the lignin extracted from PA-DES had a higher brightness than that of the native CEL. Specifically, a brightness of 22.62% ISO and 25.91% ISO was observed for L_{BDDES} and L_{EGDES}, respectively. Furthermore, L_{GLDES} possessed the highest brightness of 29.84% ISO. These results suggest that our PA-DESs, especially the GLDES system, can isolate light-color lignin whose brightness even exceeds that of native lignin. Lignin color is generally related to the chromophore content and micromorphology. Therefore, the mechanism of our PA-DES recovered lignin with a light color was revealed from the micromorphology and chemical structure, which will be illustrated later.

2.3.3. Micromorphology analysis. The micromorphology of the lignins obtained from the PA-DES fractionation was determined using FE-SEM. As shown in Fig. 2A1–C3, all lignins featured a uniform spherical shape and were termed lignin microparticles (LMPs). The average size of the LMPs varied from 550 to 3254 nm, with a narrow PDI of 0.30–0.40 depending on the type of PA-DES (Fig. 2D1–D3). Specifically, LMPs isolated by the GLDES system had the smallest average size (550 nm) and narrowest PDI (0.30), corresponding to the lightest color. The other two LMPs had much larger average sizes of 1080 nm (EGDES) and 3254 nm (BDDES). This result indicated that the PA-DES could directly generate uniform LMPs with different PAs as the HBD, which probably resulted from the structural modification with PA (*e.g.*, connecting bonds, molecular weight, and hydroxyl groups) during the fractionation process. Interestingly, it was found that the color degree ($L^*a^*b^*$ and brightness) of the LMPs was negatively correlated with the size of the LMPs, in which smaller LMPs have a lighter color. In general, LMPs with a small average size can increase the specific surface area and simultaneously enhance the interval spaces, resulting in a low bulk density. In this vein, it is likely that lignin containing similar amounts of chromophores with a low bulk density can decrease the concentration of chromophores at the macroscopic scale, thus resulting in the light color of lignin.[27]

In contrast, the CEL and lignins recovered from the organic acid-based DES by adopting the same procedures as the polyol-based DES featured irregular block-like shapes, which were wrapped by disordered lignin debris (Fig. 2E1–G3). This result suggests that our PA-DESs possess special functionalities for directly extracting lignin from lignocellulose and upgrading it into uniform LMPs. Importantly, the block-like shape of the lignin isolated from the organic acid-based DES was also associated with its dark color because of its low specific surface area and interval spaces compared with those of the LMPs.

2.3.4. Structural analysis of the isolated lignins. To better analyze the characteristics of the different DES-extracted lignins, we compared them with that of CEL, by observing them with FTIR. As shown in Fig. S3,† multiple adsorption bands were simultaneously present in the DES lignin and CEL, indicating a similar lignin structure. All the detailed signals of the FTIR spectra were identified according to previous publications.[36–38] A wide adsorption band at 3427 cm^{-1} in CEL originates from the O–H stretching vibrations of aliphatic and phenolic hydroxyl groups. Its intensity got stronger in the L_{GLDES} and L_{BDDES}, which might be induced by the grafted GL and BDO onto the α-position of the lignin sidechain, thus enhancing the aliphatic hydroxyl group contents.[39] The peaks at 2938 and 2843 cm^{-1} are ascribed to the C–H asymmetric and symmetrical stretching vibrations of the $–CH_2–$ and CH_3 groups, respectively. As expected, these peaks' intensities of L_{LADES} and L_{OADES} decreased due to the departure of formaldehyde through the C_2 route during the lignin degradation process. However, these peaks got sharpen in the L_{GLDES} and L_{BDDES}, proving that less lignin degradation through C_2 routes[40] and possible PA-grafted reactions occurred during the fractionation process. In addition, the typical adsorption peaks of other functional groups in the lignin structure can be detected, such as the stretching vibrations of unconjugated C=O groups in the carboxyl groups at 1695 cm^{-1}, aromatic ring skeletal vibrations of the phenylpropane groups at 1595, 1508 and 1419 cm^{-1}, the vibrations of C–H deformation combined with aromatic rings at 1458 cm^{-1}, the breathing

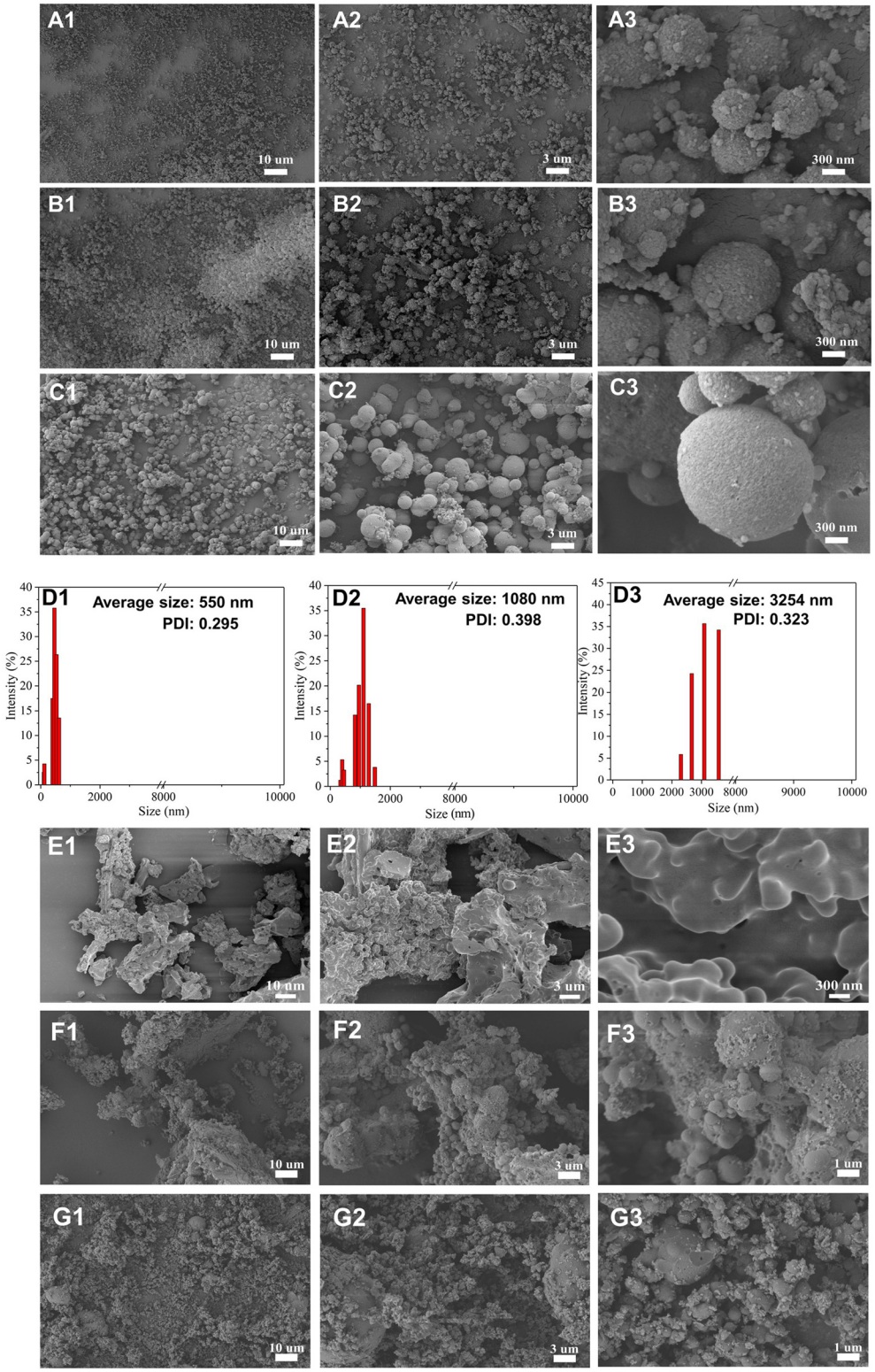

Fig. 2 SEM images of isolated LMPs and their size distribution. (A1–A3) Images of L_{GLDES}, (B1–B3) L_{EGDES} and (C1–C3) L_{BDDES} and the size distributions of (D1) L_{GLDES}, (D2) L_{EGDES} and (D3) L_{BDDES}; (E1–E3) morphology of CEL and lignins isolated from organic acid-based DES systems of (F1–F3) LADES and (G1–G3) OADES.

vibrations of syringyl and condensed guaiacyl at 1326 cm^{-1}, guaiacyl ring breathing with C–O stretching at 1267 cm^{-1}, C–C and C–O plus C=O stretching at 1219 cm^{-1}, the in-plane aromatic C–H deformation vibrations at 1028 cm^{-1}, and the C–H out-of-plane stretching at 834 cm^{-1}. All these typical absorption peaks demonstrate that the lignin extracted with a DES retained its native structure. The peak of unconjugated C=O groups (1695 cm^{-1}) was more significant in the L_{OADES}, indicating that severe lignin degradation existed in the L_{OADES}. Compared with the PA-DES, the guaiacyl peak (1267 and 1219 cm^{-1}) intensity of the L_{OADES} and L_{LADES} was stronger, indicating that more guaiacyl groups were preserved. In contrast, the peak intensity of syringyl at 1326 cm^{-1} was weaker in L_{OADES} and L_{LADES}, implying that syringyl groups degraded severely during the fractionation.

The molecular weights (M_w and M_n) and polydispersity indices (PDI) are determined to unveil the variation of lignin structures (Fig. S4†). For CEL, the M_w was 12 322 g mol^{-1}, and it significantly decreased after all the pretreatments, implying the existence of lignin depolymerization during fractionation. Specifically, PA-DES generated lignin with a high M_w in the order of L_{GLDES} > L_{EGDES} > L_{BDDES}. In contrast, lignins isolated from the organic acid-based DES had a much lower M_w of 3906 and 3026 g mol^{-1}, which are significantly lower than that of lignins isolated from the PA-DES systems. It is well known that the molecular weight of lignin is positively correlated with the content of aryl ether linkages, suggesting that our PA-DES has the unique ability to preserve the lignin structure. Notably, the color degree of lignin represented by $L^*a^*b^*$ and brightness is also positively related to its M_w, which implies that high-M_w lignin possesses fewer chromophores. In addition, the lignin recovery yield was found to be positively correlated with M_w because intact lignin can be easily recovered.[41,42] In addition, the PDI of lignin significantly decreased with decreasing M_w.

To analyze the variation of the lignin structure in the DES pretreatment, 2D-HSQC NMR was conducted, and CEL was used as a contrast. The HSQC spectrograms of the side-chain and aromatic regions of the CEL and the recovered lignins are shown in Fig. 3 and 4, and the reaction mechanism of lignin during fractionation is also proposed (Fig. 5). The main lignin cross-signals' assignment of the spectrogram was labeled according to previous publications.[43–45]

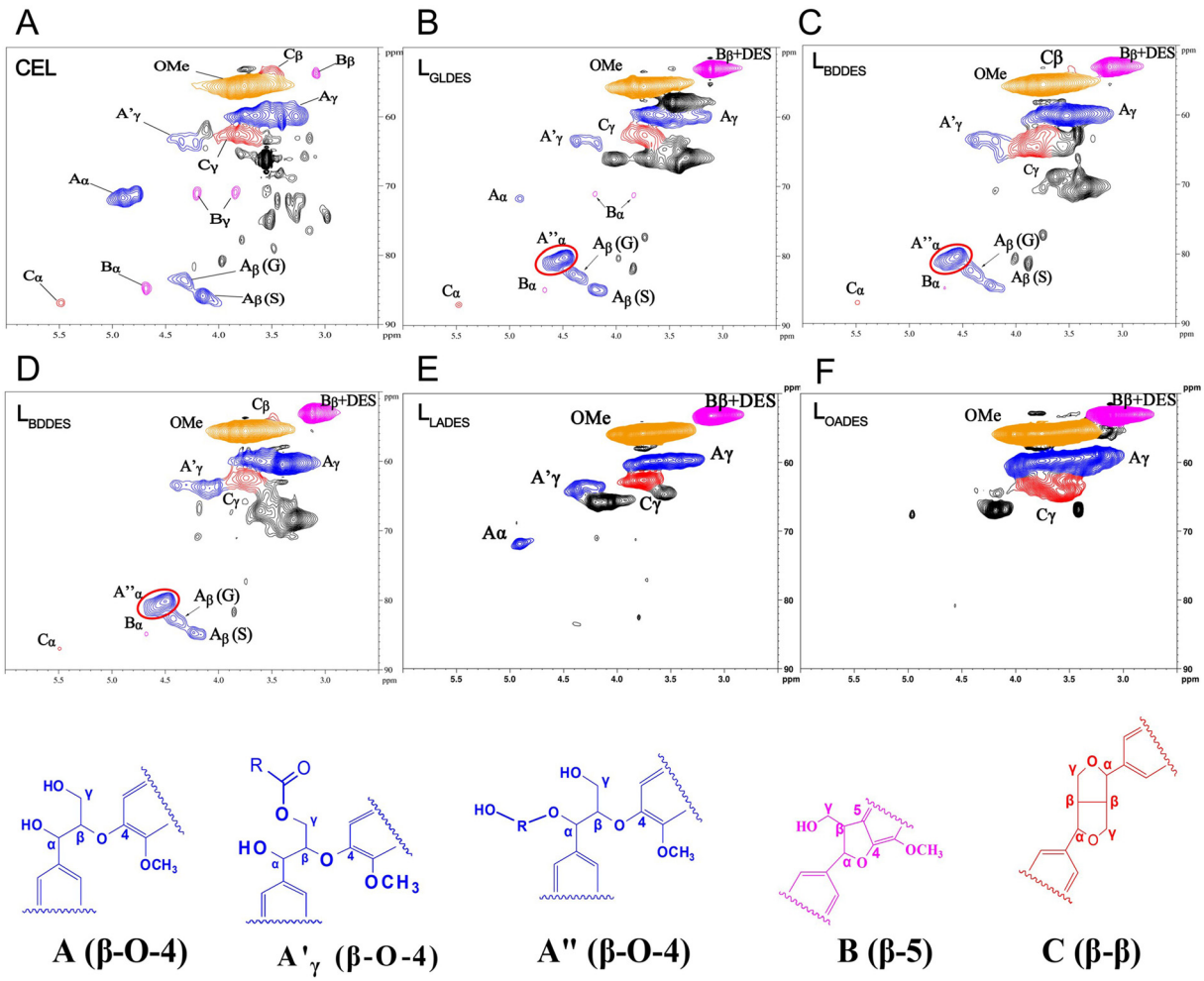

Fig. 3 $^{1}H–^{13}C$ HSQC NMR of lignin side-chain regions. (A) CEL; (B) GLDES; (C) EGDES; (D) BDDES; (E) LADES; (F) OADES.

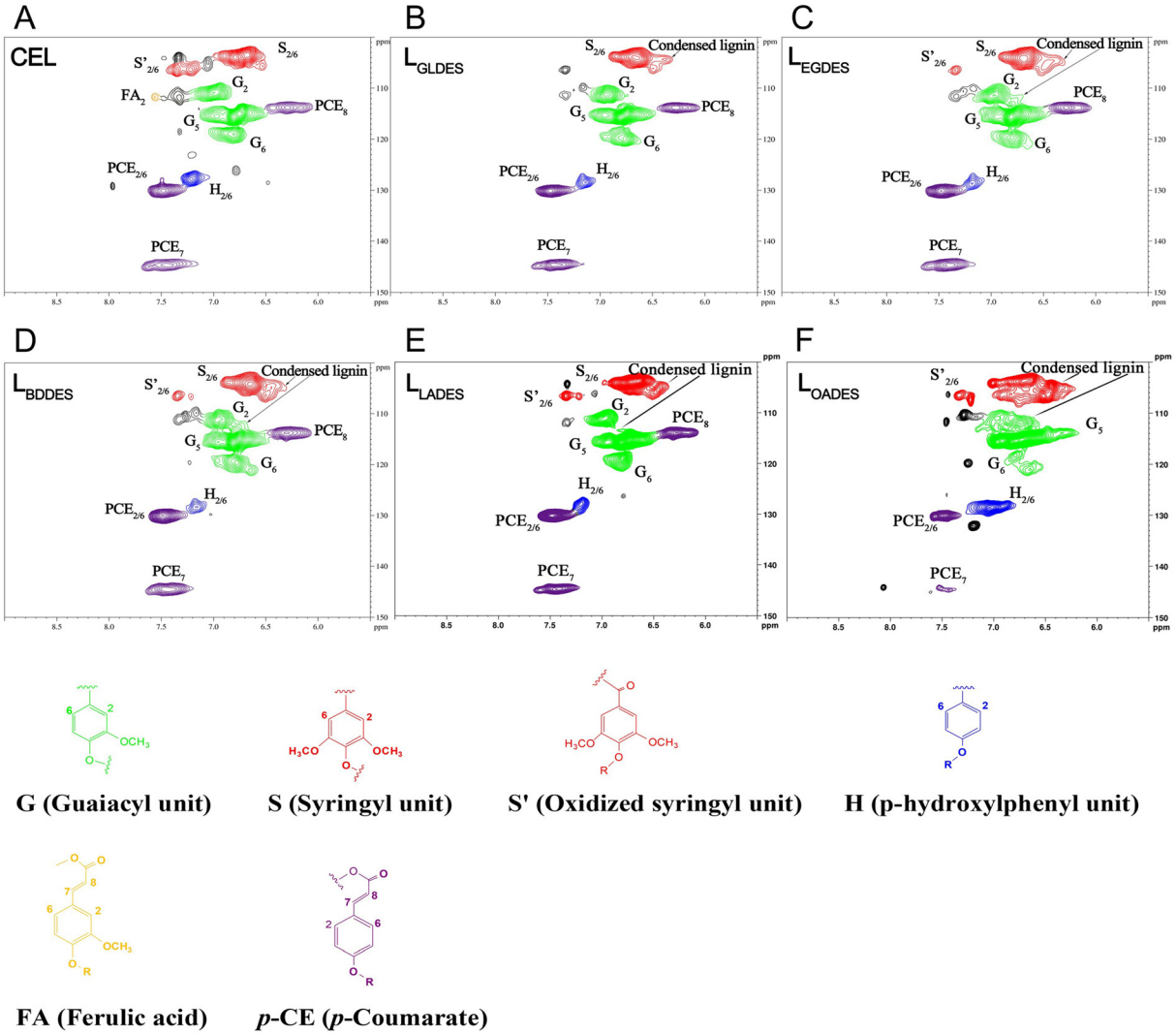

Fig. 4 ^{1}H–^{13}C HSQC NMR of lignin aromatic regions. (A) CEL; (B) GLDES; (C) EGDES; (D) BDDES; (E) LADES; (F) OADES.

The aliphatic regions (Fig. 3A) of the CEL of β-O-4 (A_α), β–β (B_α), and β-5 (C_α) exhibited strong signals at δ_C/δ_H 71.61/4.83, 84.72/4.64, and 86.85/5.40 ppm. Unambiguous signals related to β-O-4 (A_β), β–β (B_β), and β-5 (C_β) were also observed at 86.1/4.05 (A_β for S) and 83.4/4.33 (A_β for G), 53.5/3.05, and 52.4/3.45 ppm, respectively. The γ-position of β-O-4 (A_γ), β–β (B_γ), and β-5 (C_γ) signals was centered at 59.5/3.69, 71.0/4.16–3.79, and 62.3/3.70 ppm, respectively. A signal belonging to γ-acetylated β-O-4 linkages (A'_γ) was clearly recognized,[12] implying that the LCC structure exists in bamboo. The quantification of CEL and the isolated lignins is shown in Table 1. In CEL, the β-O-4 linkages' content was 59.19/100Ar, and it greatly reduced after the PA-DES fractionation, which ranged from 13.76 (L_{GLDES}) to 9.36 (L_{EGDES}) and 4.73/100Ar (L_{BDDES}), indicating that the β-O-4 linkages' content was greatly determined by the type of PA-DES. With the reduction of the signal of β-O-4 linkages, a strong signal at 80.05/4.49 ppm appeared, which was ascribed to the PA-functionalized β″-O-4 (A''_α) through α-OH etherification in the lignin side chains (see the red circles in Fig. 3B–D). Notably, this functionalization resulting from PA could significantly stabilize the β-O-4 linkages in lignin, protect it from degradation during fractionation, and efficiently inhibit lignin repolymerization reactions.[39,46] This functionalization made the total β-O-4 linkages (A_α and A''_α) maintained as high as 52.51 (L_{EGDES})–58.01/100Ar (L_{GLDES}) which equivalently account for 88.71–98.01% of the CEL. It is widely acknowledged that β-ether cleavage is accompanied by the generation of potential chromophores of phenolic hydroxyls, which can be readily converted into ketones, aldehyde and quinoid structure.[47] The existence of these structures is regarded as one of the dominant reasons for the darkening of lignin.[48] Notably, lignin protection by PA could significantly hinder the formation of phenol hydroxyl, thus greatly restricting the formation of phenol hydroxyl and avoiding the dark color of lignin. The other C–C linkages, including β–β and β-5, slightly decreased after PA-DES fractionation, indicating that

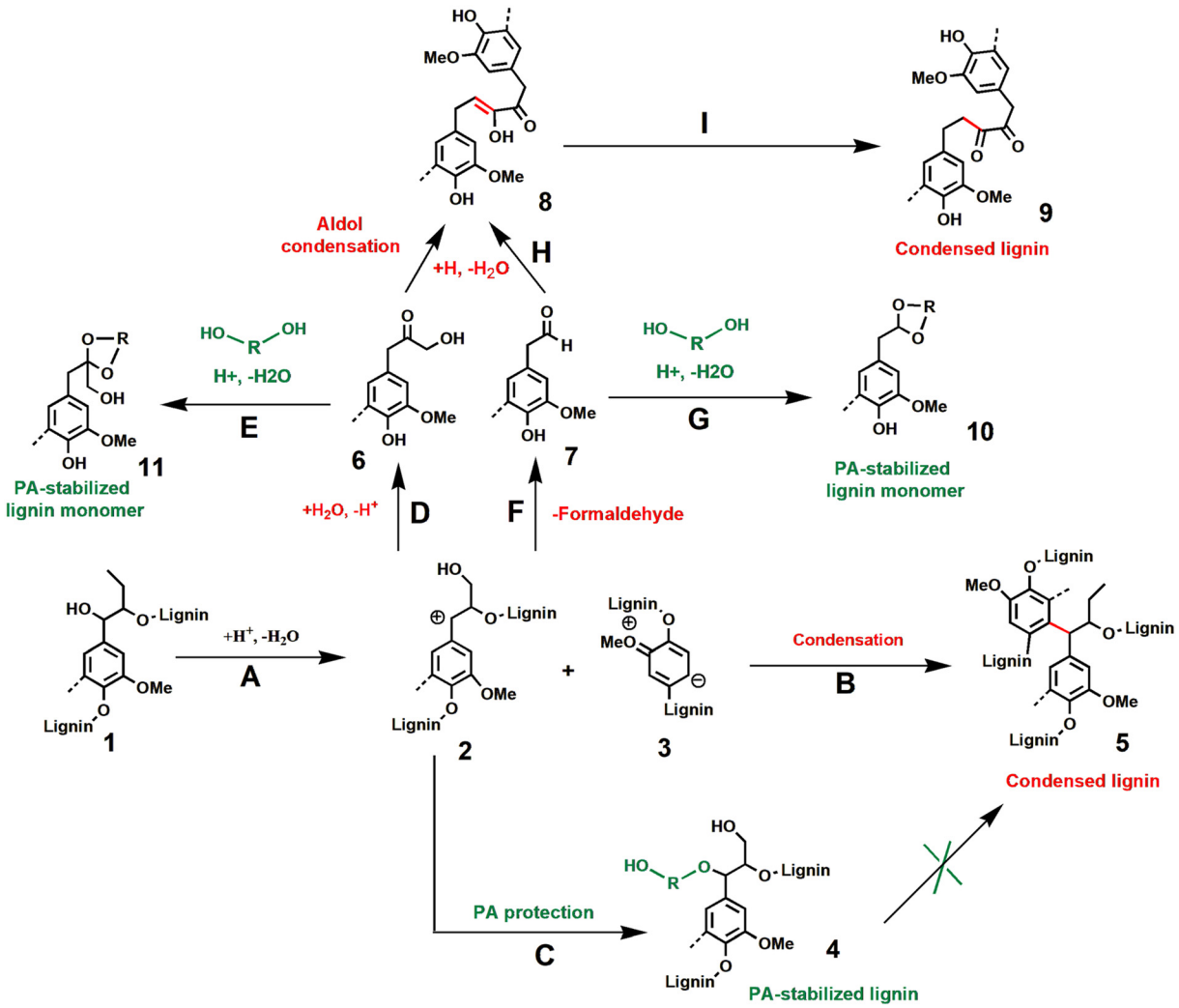

Fig. 5 Mechanisms of lignin degradation and PA stabilization.

Table 1 Quantification of CEL and isolated lignins (per 100Ar) by HSQC NMR

		S (%)		G (%)					
Sample	Lignin removal (%)	Total	Condensed	Total	Condensed	S/G	β-O-4 (%)	β″-O-4 (%)	Total β-O-4 (%)
CEL	—	43.39	0	45.82	—	0.95	59.19	0	59.19
L_{EGDES}	55.07	49.23	8.83	43.98	3.20	1.12	9.36	43.15	52.51
L_{GLDES}	66.20	48.42	7.82	47.70	1.52	1.10	13.76	44.25	58.01
L_{BDDES}	70.63	53.52	9.32	40.81	2.58	1.31	4.73	48.52	53.25
L_{LADES}	34.56	50.92	8.28	41.71	2.51	1.22	28.49	0	28.49
L_{OADES}	42.32	38.77	24.72	43.56	43.56	0.89	0	0	0

the C–C linkages were stable during the treatment (Table S5†). Moreover, the β-ether content in the recovered L_{LADES} greatly decreased to 28.49/100Ar and was absent in L_{OADES}. As for the C–C linkages, the β–β and β-5 in L_{LADES} decreased to 2.46 and 4.21/100Ar, respectively, and both of them finally disappeared in L_{OADES} (Table S5†). These results implied that β-ether and other C–C linkages could be easily cleaved without PA protection. Significant β-ether cleavage greatly facilitated the generation of potential conjugated chromophores of aldehyde-containing monomers and Hibbert's ketone, which could be converted into conjugated chromophores by aldol condensation,[40] thus darkening the color of lignin.

To clarify lignin functionalization, a mechanism was proposed, as shown in Fig. 5. In common acid fractionation systems, a carbocation at the α-position of lignin side-chains can be easily formed by H^+ attack (process A in Fig. 5), which partially results in condensation reactions with the adjacent lignin fragments.[49] Furthermore, β-ether acidolysis occurs

mainly *via* two pathways: one leads to the cleavage of C_β–C_γ with aldehyde-containing lignin fragments and formaldehyde (C_2 pathway of F) and the other forms Hibbert's ketone lignin fragments (C_3 pathway of D) under acidic conditions. Both types of carbonyl monomers may undergo further aldol condensation (pathway H) or condensation with C_2 or C_6 on the lignin aromatic rings.[40] During these β-ether cleavage and condensation reactions, the formation of the conjugated C=O and C=C structures (products 8 and 9 in Fig. 5) might be the pivotal reason for the darkening of lignin in most acid fractionation processes, including the contrastive systems of LADES and OADES in this study. In the PA-DES process, PA can readily graft onto the α-position of the carbocation intermediates (pathway C), thus significantly hindering the cleavage and condensation reactions of the β-ethers and leading to an intact lignin structure with low chromophores, such as CEL. Although minor β-ether of lignin might undergo acidolysis by C_2 and C_3 parthways during PA-DES fractionation, PA (*e.g.*, EG) could also stabilize the acidolysis products or inherent carbonyl groups through acetal protection (pathways E and G, Fig. 5), thus quenching the potential chromophoric carbonyl groups. Overall, the significant protection induced by PA could result in an intact lignin structure which has almost no chromophore formation during fractionation, thus leading to light-color lignin.

In the aromatic regions (Fig. 4A), signals of the guaiacyl (G), syringyl (S), oxidized syringyl (S′), and *p*-hydroxyphenyl (H) units were clearly observed in the CEL. In addition, ferulate (FA) and *p*-coumarate (PCE) signals were clearly identified. The cross peaks of $S_{2,6}$ and $S'_{2/6}$ were located at δ_C/δ_H 104.0/6.72 and 106.3/7.21 ppm. The signals ascribed to guaiacyl (G) were at 111.0/6.97 ppm (G_2), 114.8/6.69 ppm (G_5), and 119.1/6.81 ppm (G_6). The *p*-hydroxyphenyl (H) signal was located at δ_C/δ_H 127.9/7.19 ppm ($H_{2,6}$). After PA-DES fractionation, the $S_{2/6}$ signals showed no distinct shifts. Specifically, only a small amount of condensed S units was found throughout the fractionation, ranging from 7.82/100Ar (L_{GLDES}) to 9.32/100Ar (L_{BDDES}). It was even negligible throughout the PA-DES pretreatment for the condensed G units (1.52–2.58/100Ar). The small amounts of condensation reactions suggested that our PA-DES could preserve the lignin structure well, thus obtaining a light-color lignin similar to CEL. The S/G ratio increased slightly from 0.95 to 1.31, suggesting that G units were easily reacted during the treatment. In addition, the H units decreased after PA-DES fractionation. As for the FA content, representing the variation of LCC linkages, it disappeared after PA-DES fractionation, while the PCE remained nearly constant (Table S5†). These results may be due to significant hemicellulose degradation during pretreatment. In contrast, L_{LADES} also had low amounts of condensed G (2.51/100Ar) and S (8.28/100Ar), which might be ascribed to its limited lignin isolation (only 34.56% lignin removal) at 110 °C for 3 h. When fractionation occurred in a relatively harsh OADES system, the condensed S units dramatically increased to 24.72/100Ar, whereas the G units completely condensed (43.56/100Ar). Condensed lignin containing conjugated C=O and C=C structures with phenolics might be mainly responsible for the dark color of lignin.[38] In addition, the H unit content of the L_{OADES} increased significantly, while the PCE decreased significantly (Table S5†). This result might have resulted from the PCE transformation into H units, indicating that the lignin structure changed significantly during fractionation.

The OH contents, including aliphatic, phenolic, C_5 substituted (syringyl and other types of condensed 5-substituted), and carboxylic acid, were quantified by lignin phosphorylation followed by ^{31}P NMR. As illustrated in Fig. 6A, the aliphatic OH content in CEL was 3.61 mmol g^{-1}, accounting for 72.17% of the total OH groups. After PA-DES fractionation, it slightly decreased and ranged from 2.69 (L_{BDDES}) to 2.95 mmol g^{-1} (L_{GLDES}), but was still predominant in the total OH contents (66.33%–67.17%). In addition, the phenolic OH content in CEL was 1.18 mmol g^{-1}, accounting for 23.61% of the total OH. After pretreatment, the total phenolic OH increased negligibly and was maintained at ~1.25 mmol g^{-1}, suggesting that there was no extra generation of phenolic OH during our PA-DES fractionation. This result is also consistent with the 2D HSQC NMR results, implying that our PA-DES could significantly constrain the generation of potential chromophoric groups through PA etherification stabilization. In contrast, the aliphatic OH in L_{LADES} and L_{OADES} is much lower than the lignin recovered from PA-DES, which is 1.38 and 0.94 mmol g^{-1}, respectively. However, the total phenolic OH of both L_{LADES} (1.86 mmol g^{-1}) and L_{OADES} (2.73 mmol g^{-1}) is much higher than that of PA-DES' lignin. These results imply that lignin isolation without PA protection in common organic acid DESs will result in a great increase in the potential chromophore of phenolic OH with a substantial sacrifice of the β-O-4 ether bonds. In addition, the C_5-condensed OH in these acidic systems was far beyond that of the PA-DES system, suggesting severe condensation reactions during fractionation. The increased lignin condensation, including the possible aldol condensation of lignin debris containing the conjugated C=O and C=C structures, might be one of the main reasons for the enhancement of lignin color.

It is widely acknowledged that conjugate structures in lignin determine the color of lignin, whether yellow, brown, or dark. These groups mainly include conjugated phenolic-, furan- and quinone structures,[25] as can be seen in Fig. 6C. Among the known chromophores in lignin, nearly all of them possess carbonyl groups; thus, we quantified the carbonyl groups including ketone, aldehyde, and quinone of the CEL and recovered lignins by derivatization with 4-(trifluoromethyl) phenylhydrazine, followed by ^{19}F NMR (Fig. 6B) to better explain the reason for the light-color lignin. It can be seen that the ketone, aldehyde and quinone groups in CEL were 0.31, 0.25 and 0.74 mmol g^{-1}, respectively. After GL- and EGDES isolation, each of these groups reduced, in which the L_{GLDES} possessed the lowest carbonyl contents of 0.13 (ketone), 0.11 (aldehyde) and 0.47 mmol g^{-1} (quinone), with a total carbonyl content of 0.70 mmol g^{-1}, indicating that our PA-DES could quench the inherent carbonyl chromophores during its isolation. For L_{BDDES}, the carbonyl groups were almost unchanged

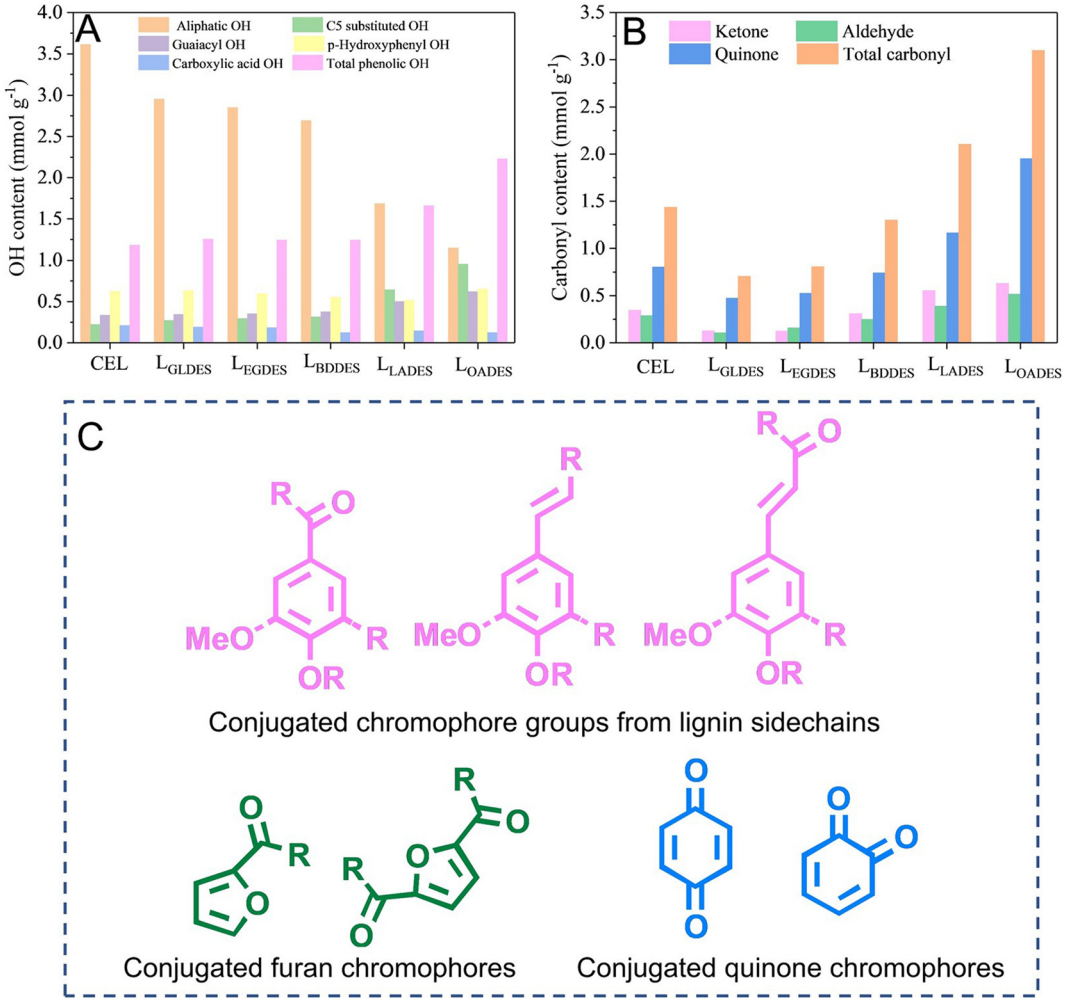

Fig. 6 ^{31}P and ^{19}F quantification. (A) Hydroxyl groups, (B) carbonyl groups of CEL and isolated lignins, and (C) common chromophore groups in lignin.

and very close to the CEL. In the case of the acid DES (LA- and OADES), the total carbonyl content of the dark-color lignins recovered from the organic acid-based DES of L_{LADES} and L_{OADES} was 2.10 and 3.10 mmol g^{-1}, respectively, far beyond that of the lignins isolated from the PA-DES systems. As expected (Fig. S5†), the brightness of lignins had a significant negative correlation with the carbonyl group content of ketones (R^2 = 0.94), aldehydes (R^2 = 0.92), quinones (R^2 = 0.84), and total carbonyl groups (R^2 = 0.90), suggesting that carbonyl-derived chromophores were the main reason for the dark color of lignin.

Overall, the carbonyl-conjugated chromophore groups generated by aldol condensation during the conventional lignin isolation processes mainly contribute to the dark color of the lignin. This study successfully hindered the cleavage of β-ethers and aldol condensation reactions *via* PA-grafting reactions to avoid the generation of chromophoric groups of phenolic conjugated C=O and C=C structures, as well as the potential chromophores of phenolic OH groups or quenching of the inherent chromophores of natural lignin in lignocellulose, thus yielding a light-color lignin. In contrast, dark-color lignins isolated from the organic acid-based DES systems without PA protection showed severe cleavage of β-O-4 linkages, lignin condensation, and increased carbonyl content, especially in the OADES system, generating more chromophoric groups and resulting in darker-color lignins. Notably, this process proposed a low-cost production method for obtaining light-color lignin with a well-preserved structure, significantly lower than the conventional MWL.

2.4. UV-protecting properties of light-color LMPs

Considering the highest brightness of lignin recovered from the GLDES system, we chose L_{GLDES} for testing its application as a sunscreen agent. The light-color lignin used in sunscreen was investigated by mixing it with pure cream or commercial SPF 15 sunscreen. As shown in Fig. 7A, the color of the prepared sunscreen with the naked eye slightly increased from white (1 wt% addition) to pale yellow (5 wt% addition) as the lignin content increased, while all these colors were close to our human skin, thus satisfying the makeup requirements. As

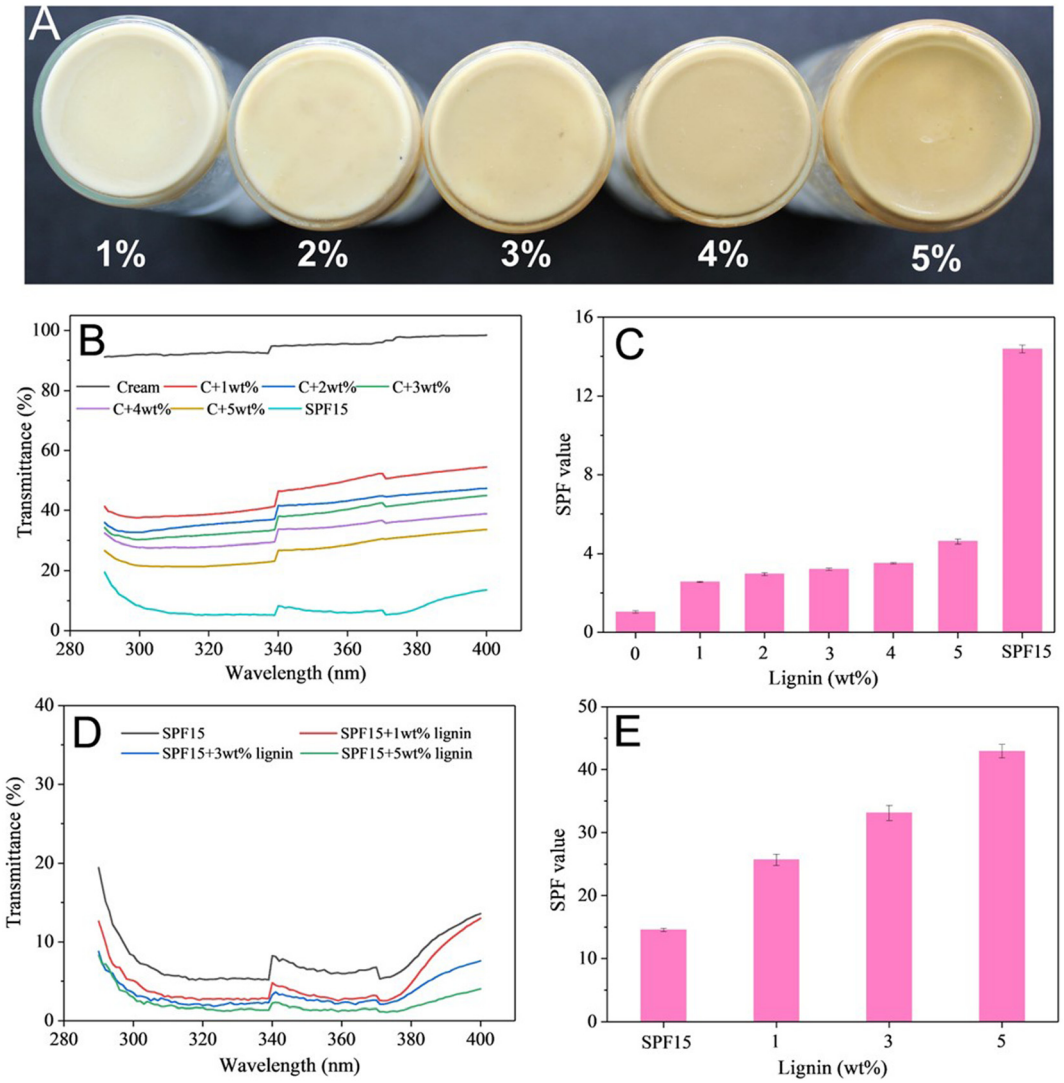

Fig. 7 Morphology of the sunscreens and their SPF values. (A) Digital photographs of the pure cream with different LMP additions; (B) UV transmittance of the pure cream and lignin-added sunscreens with different amounts of lignin addition and (C) their corresponding SPF values; (D) UV transmittance of the commercial SPF 15 sunscreen and lignin-added SPF 15 sunscreens with different lignin contents and (E) their corresponding SPF values.

for the sun protection properties (Fig. 7B and C), the pure cream had almost no absorbance in the UV (290–400 nm) area and its corresponding SPF was only 1.04. As lignin was introduced into the pure cream, the UV transmittance declined and its corresponding SPF value was significantly enhanced. The transmittance decreased with increasing lignin loading. As the lignin content increased to 5%, the transmittance of the lignin sunscreen in the UVA (320–400 nm) and UVB (290–320 nm) areas was lower than 30%, and the SPF value was enhanced to 5.11 (Fig. 7C), ~5 times higher than that of pure cream, indicating that the light-color L_{GLDES} is a very good natural candidate for sunscreen.

Although having excellent sunscreen performance in pure cream, it still cannot match the SPF values of the commercial sunscreen; therefore, we added L_{GLDES} to the commercial SPF 15 sunscreen to enhance its performance, in order to rival commercial SPF 30 or SPF 50. For the commercial SPF 15 (Fig. 7D), the UV transmittance of the partial regions of UVA (386–400) and UVB (290–297) was still over 10%, while it significantly declined as the lignin addition increased, and all of them decreased to <8% with the addition of 5% lignin. As shown in Fig. 7E, the commercial SPF 15 sunscreen had an SPF value of 14.57, which dramatically enhanced to 25.72 (1% lignin addition) and exceeded common commercial SPF 30 after 3% lignin addition with SPF of 33.11. When the lignin content was further increased to 5%, the SPF value reached 42.91. In a previous study, the SPF value easily reached a plateau or even declined with increasing lignin addition because of its poor dispersity.[50] In this study, the SPF continually increased to as high as 42.91 with an increase in lignin content. This result might be due to the excellent dispersibility of the regular spherical microspheres in our L_{GLDES}.

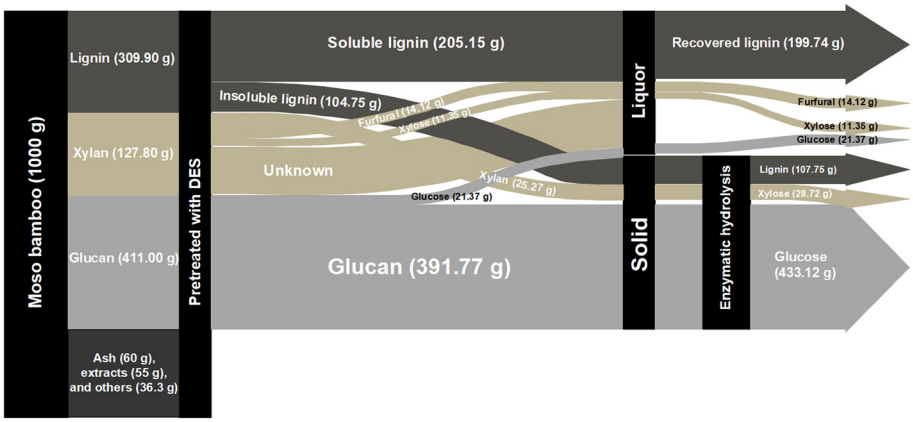

Fig. 8 Mass balance diagram of the GLDES fractionation system.

2.5. Biorefining mass balance

Mass balance was performed using 1000 g of raw biomass as the starting feedstock using the GLDES system at the fractionation temperature of 110 °C for 1 h. As shown in Fig. 8, 586.28 g cellulose-rich solid was recovered after the fractionation, which contained 391.77 g glucan, 25.27 g xylan and 107.75 g lignin. The subsequent enzymatic saccharification process yielded 433.12 g glucose and 28.72 g xylose which could be converted into fuels and chemicals. In addition, 205.15 g of lignin was isolated and 199.74 g of light-color lignin microspheres with a 97.36% lignin recovery yield were obtained using a simple antisolvent method, which possessed a conspicuous UV shielding performance as a sunscreen agent. In the fractionation liquor, 11.35 g xylose and 14.12 g furfural were quantified, which could also be isolated and converted into fuels and chemicals.

3. Future prospective

Although the light-color lignin possesses an excellent performance as a sunscreen agent, its other natural properties such as antibacterial and antioxidant are also meaningful to be investigated. In addition, the relationship between lignin structure and the activity of animal cells should also be further studied to expand the high-value application in human life. Apart from lignin utilization as the sunscreen and cellulose saccharification upgrading, the degraded 80 wt% xylan should also be processed into valuable chemicals and fuels. Therefore, the degradation routes and the mechanism of xylan should also be investigated to provide a reliable theory to design a feasible route for xylan valorization.

4. Conclusion

The potential of lignin as a dye dispersant or sunscreen additive facilitates its high-value valorization. However, current lignin fractionation methods focus too much on delignification while neglecting the lignin quality, forming large amounts of chromophores that darken the lignin. Researchers have tried various methods to whiten lignin, while low yield, complicated processes and even using toxic chemicals still limit the application of lignin. Herein, we first proposed a sustainable polyol-DES fractionation system directly using lignocellulose biomass as the starting feedstock for the preparation of light-color lignin, which innovatively combined chemical stabilization and morphological modification in "one pot" for the reduction of chromophores. The recovered lignin possessed 29.84% ISO whiteness with a regular microspherical morphology, a high recovery yield (97.36%), enriched β-ether linkages of 58/100Ar, a low phenolic hydroxyl content of 1.25 mmol g^{-1}, a minimal C=O content of 0.70 mmol g^{-1} and a less condensed structure. The mechanism for the generation of light-color lignin was systematically analyzed. The recovered lignin showed excellent performance in sunscreen applications, which could easily enhance the sun protection factor of commercial SPF 15 to SPF 40 with the addition of 5 wt% lignin. The recovered cellulose-rich residue obtained 99.47% enzymatic saccharification yield, which could be further converted into fuels. Overall, this study elucidated the mechanism for obtaining light-color lignin while simultaneously enhancing the enzymatic saccharification yield, which could provide an essential reference for producing light-color lignin and digestible cellulose.

5. Materials and methods

5.1. Materials

Bamboo (Phyllostachys edulis) harvested in Zhejiang Province (China) was processed into chips in a local pulping factory. After being received, the bamboo chips (~50 mm length, 30 mm width and 7 mm thickness) were washed and immersed in DI water overnight, and then subjected to fibrillation using a twin-screw extruder. Finally, the fragmented feedstock (~1 mm length and 10 μm width) was air-dried and transferred to a bag for further use. Cellulase (Cellic® CTec2,

Novozymes, 250 FPU g^{-1}) and xylanase (X2753-50g, 3490 U g^{-1}) were obtained from Sigma-Aldrich (Shanghai, China). Pure NEVEA soft moisturizing cream (75 mL) and Curél SPF 15 sunscreen were purchased from Alibaba. Choline chloride (ChCl), ethylene glycol (EG), glycerol (GL), 1,4-butanediol (BD), $AlCl_3$, oxalic acid (OA), lactic acid (LA) and ethanol were ordered from Sinopharm Chemicals (Beijing, China).

5.2. DES synthesis, pretreatment, and LMP formation

DESs were synthesized in a three-neck flask using a glycerin bath by weighing ChCl, polyhydric alcohols (PA), and $AlCl_3$ at a molar ratio of 25 : 50 : 1 with constant stirring at 200 rpm until a transparent and homogeneous liquid was formed at 90 °C. In addition, organic acid-based DESs, including oxalic acid (OA)- and lactic acid (LA)-based DESs, were prepared by mixing ChCl and organic acids at a molar ratio of 1 : 2 using the same procedures. According to the variety of HBDs, the DES systems were shortened to EGDES (ChCl/EG/$AlCl_3$), GLDES (ChCl/GL/$AlCl_3$), BDDES (ChCl/BD/$AlCl_3$), OADES (ChCl/OA), and LADES (ChCl/LA), respectively. Detailed procedures could be found in a previous publication.[51]

For the treatment process, 10 g of dry bamboo was blended with 100 g of DES at the target temperatures of 100–120 °C at a heating rate of 2 °C min^{-1} with constant stirring for 1 h. Notably, considering the poor lignin isolation of the LADES system,[22] the LADES pretreatment was conducted for 3 h at 110 °C. At the end of each reaction, 300 mL of ethanol/water (1 : 1, v : v) was poured into the reactor to terminate the treatment, and the mixture was transferred into a beaker and magnetically stirred for 2 h. Next, the solid and liquid were separated by vacuum filtration, after which 200 mL of fresh ethanol solution was added to wash the solid thrice. The collected lignin-rich liquid was then evaporated to remove ethanol, and 500 mL of water was added to precipitate and recover the lignin. After being washed with excess DI water to neutral pH, lignin was finally obtained by freeze-drying.

5.3. Enzymatic saccharification

Enzymatic saccharification was performed in 150 mL flasks by adding substrates, cellulase (25 FPU per g-glucan), xylanase (150 U per g-xylan), acetate buffer (pH ~ 4.8), and DI water at a substrate concentration of 2.5%. The flasks were incubated in a shaker (50 °C, 150 rpm) for 72 h. At the end of the incubation, 1 mL of liquid was sampled, diluted, and analyzed by high-performance liquid chromatography (HPLC).

5.4. Characterization of the DES solvents

The viscosity of the DESs was determined at different temperatures, including 30, 60, 90 and 110 °C. The reported viscosity was the average value of four measurements and was measured with a viscosity meter according to previous publication.[21,29]

The KamLet-Taft empirical parameters (*e.g.*, α, β, π^*) of the DESs, which quantified the hydrogen-bond donating ability (acidity), hydrogen-bond accepting ability (basicity) and polarity of the solution, were determined by solvatochromic parameter measurements.[29,52,53] The corresponding dyes were first dissolved in methanol with a concentration of 1.0×10^{-3} mol L^{-1}. The dye solution (50 μL) was transferred into a centrifuge tube. After removing the methanol in a vacuum-drier (40 °C, 40 min), 2.0 g DES was introduced into the centrifuge tube with ultrasonication for 20 min to form a homogeneous dye–DES solution. Subsequently, the generated dye–DES solution was put into a quartz cell with 1.0 cm light path length. The adsorption spectra were recorded on a UV-vis spectrophotometer at 25 °C.

Nile red was used to determine the value of π^*, which was calculated on the basis of the following equation:

$$\pi* = (19.839 - \nu_{NR})/2.9912$$

In this equation, $\nu_{NR} = 1/[\lambda_{(NR)\ max} \times 10^{-4}]$, where $\lambda_{(NR)\ max}$ represents the maximum absorption wavelength of Nile red.

For determining the value of β, 4-nitroaniline was employed, and the β value was calculated using the following equation:

$$\beta = 11.134 - \frac{3580}{\lambda_{(NH_2)\ max}} - 1.125 \times \pi^*$$

In this equation, $\lambda_{(NH_2)\ max}$ is the maximum absorption wavelength of 4-nitroaniline.

For determining the value of α, Nile red was used, and the α value was calculated using the following equation:

$$\alpha = 19.9657 - 1.0241 \times \pi* - \nu_{NR}/1.6078$$

5.5. Characterization of the lignin

The lignin recovery yield was calculated according to the extracted lignin in the liquid, and the corresponding equation is as follows:

$$\text{Lignin yield}\ (\%) = \frac{\text{Lignin recovered from the treatment liquid (g)}}{\text{Total removed lignin from the initial substrate (g)}} \times 100\% \quad (1)$$

Sugar analysis of the recovered lignin was conducted using the NREL (National Renewable Energy Laboratory) protocol as previously described.[51] Cellulolytic enzyme lignin (CEL) was obtained following a ball-milling, enzymatic digestibility and dioxane extraction process.[42]

FTIR (Fourier transform infrared) was applied to characterize the functional groups of the CEL and isolated lignins. The test was conducted using a Bruker TENSOR27 spectrometer in transmittance mode with 32 scans at 4 cm^{-1} resolution over the wavenumber range of 4000–400 cm^{-1}. Elemental analysis of the CEL and recovered lignin was performed using an elemental analyzer (Unicube, Elementar, Germany). All samples were tested three times and the mean values were calculated as the final data.

The lignin bulk density was tested in a 5 mL cylinder according to a previous publication.[27] The bulk density was obtained based on the weight of the lignin and the recorded volume. The color of the recovered lignin was analyzed using digital photographs, and its brightness was quantitatively

measured using an L&W brightness and brightness tester (Elrepho 070, Sweden). The tested items contained brightness and CIE $L^*a^*b^*$ values.[54] The micro-morphology variations of the recovered lignins were observed by field-emission scanning electron microscopy (FE-SEM, S-3400N II, HITACHI Company, Japan). Prior to the test, the lignins were taped onto electronic conductive tape and sprayed with gold. The average size (Z-ave) and size distribution of the LMPs were analyzed using a Zetasizer (Nano ZS, Malvern Instruments, UK). Before the analysis, the lignin samples were homogeneously dispersed in DI water (1 g L^{-1}) by sonication for 10 min.

The molecular weight of the lignin was quantified by gel permeation chromatography (GPC, Agilent, USA). Before the test, lignin was acetylated using pyridine/acetic anhydride (1 : 1, v : v) by magnetic stirring for 24 h. The acetylated lignins were then THF-dissolved and analyzed by GPC using a UV detector at 260 nm. Lignin samples (~150 mg) for two-dimensional ^{1}H–^{13}C (2D) Heteronuclear Single-Quantum Correlation (HSQC) Nuclear Magnetic Resonance (NMR) analysis were prepared by being dissolved in DMSO-d_6 (0.6 mL). For quantification of hydroxyl groups by ^{31}P NMR, ~20 mg of dried lignin was mixed with 0.4 mL anhydrous pyridine and deuterated chloroform (1.6 : 1, v/v) to form a solution in an NMR tube, and then 0.15 mL of a mixed solution containing an internal standard (cyclohexanol) and relaxation agent (chromium acetylacetonate) was injected with a Hamilton syringe. Before the test, an excess phosphitylation reagent (~0.1 mL of 2-chloro-4,4,5,5-tetramethyl-1,3,2-dioxaphospholane) was introduced to react with the solution. For the ^{19}F NMR test, lignin was first derivatized with 4-(trifluoromethyl) phenylhydrazine. Briefly, ~60 mg of lignin was weighed into a flask, followed by the addition of 1 mL of DMF/water (v : v, 1 : 1) solvent containing 110 mg of 4-(trifluoromethyl) phenylhydrazine. After stirring for 24 h at RT in the dark, the lignin was precipitated by introducing 20 mL of hydrochloric acid (pH ~ 2.0) and then frozen. Upon melting, the derivatized lignin was washed, recovered by centrifugation, and then vacuum-dried at 50 °C for 24 h. The dried samples were dissolved in 0.6 mL DMSO-d_6 containing an internal standard (3-trifluoromethoxybenzoic acid, 10 mg mL^{-1}) and external standard (hexafluorobenzene, 10 mg mL^{-1}). 2D HSQC NMR, ^{31}P NMR and ^{19}F NMR were performed using a Bruker AscendTM 600 MHz spectrometer, and the detailed sample preparation procedures and acquisition parameters were obtained from previous publications.[51,55,56]

5.6. Substrate characterization

The compositions of the raw and recovered substrates were analyzed by two-stage acid hydrolysis using the NREL protocol.[57] Glucan, xylan and lignin were separated by sequential concentrated and diluted acid hydrolysis. The glucan and xylan were hydrolyzed into glucose and xylose and quantified by HPLC. The soluble lignin was determined by analyzing the hydrolysis liquid using an ultraviolet spectrophotometer at 205 nm, and the content of insoluble lignin (Klason lignin) was obtained in a muffle furnace at 600 °C for 24 h.

5.7. Preparation of LMP sunscreen samples and determination of sun protection factor (SPF)

All the LMP based sunscreens were prepared by blending the LMPs (1–5 wt% addition) and pure cream with constant magnetic stirring.[50] For example, 1 wt% LMP sunscreen was synthesized by mixing 0.01 g LMPs and 0.99 g cream at 200 rpm for ~5 h in a dark room at RT. For SPF measurement, transparent tape was attached to a clear quartz slide with a thickness of 2 mm, and the experimental area was 12.5 cm^2 using a 2 mg cm^{-2} sunscreen loading, according to a previous publication.[50] Prior to the test, each sample was dried for 15 min in the dark. For each sunscreen cream, a minimum of six non-overlapping spots were selected for UV transmittance measurement using UV-8000 (METASH, China) per nm in the wavelength range of 290–400 nm in the transmittance mode (T). The SPF value was calculated using the following equation:

$$\mathrm{SPF} = \sum_{290}^{400} E_\lambda S_\lambda \Big/ \sum_{290}^{400} E_\lambda S_\lambda T_\lambda \quad (2)$$

where E_λ is the erythemal spectral effectiveness, S_λ is the solar spectral irradiance, and T_λ is the spectral transmittance of the sample.

Author contributions

J. Y. C., C. H. designed research; J. Y. C., C. H., X. L. Z., C. X. H., and G. G. F. performed research; J. Y. C., C. H., C. G. Y., X. Z. M., and A. J. R. wrote and reviewed the manuscript.

Data availability

The authors declare that the data supporting the findings of this study are available within the paper and the ESI.†

Conflicts of interest

The authors declare that they have no competing interests.

Acknowledgements

This work was supported by the National Natural Science Foundation of China (32371821, 32301546), the Fundamental Research Funds of CAF (CAFYBB2023QA006), the National Key Technology Research and Development Program of China (2023YFD2201904), the Jiangsu Province Key Laboratory of Biomass Energy and Materials (JSBEM-S-202203), and the Young Elite Scientist Sponsorship Program by CAST. The AJR and XM efforts were supported by the University of Tennessee, Knoxville.

References

1 S. Bertella and J. S. Luterbacher, *Trends Chem.*, 2020, **2**, 440–453.
2 Y. M. Questell-Santiago, M. V. Galkin, K. Barta and J. S. Luterbacher, *Nat. Rev. Chem.*, 2020, **4**, 311–330.
3 I. Leppänen, T. Lappalainen, T. Lohtander, C. Jonkergouw, S. Arola and T. Tammelin, *Nat. Commun.*, 2022, **13**, 1814.
4 A. J. Ragauskas, G. T. Beckham, M. J. Biddy, R. Chandra, F. Chen, M. F. Davis, B. H. Davison, R. A. Dixon, P. Gilna, M. Keller, P. Langan, A. K. Naskar, J. N. Saddler, T. J. Tschaplinski, G. A. Tuskan and C. E. Wyman, *Science*, 2014, **344**, 1246843.
5 C. Cai, N. Li, H. Liu, J. Zhang, J. Y. Zhu and F. Wang, *Chem. Eng. J.*, 2023, **453**, 139730.
6 P. P. Thoresen, L. Matsakas, U. Rova and P. Christakopoulos, *Bioresour. Technol.*, 2020, **306**, 123189.
7 Z. Pan, Y. Li, Z. Zhang, F. Xu, S. Ramaswamy, A. Abdulkhani and X. Zhang, *Ind. Crops Prod.*, 2022, **186**, 115173.
8 J. Lu, M. Cheng, C. Zhao, Q. Shao and M. Hassan, *Bioresour. Technol.*, 2021, **343**, 126085.
9 Z. Li, C. Chen, R. Mi, W. Gan, J. Dai, M. Jiao, H. Xie, Y. Yao, S. Xiao and L. Hu, *Adv. Mater.*, 2020, **32**, 1–8.
10 C. Zhang, X. Shen, M. Liu, J. Wen and T. Q. Yuan, *ACS Sustainable Chem. Eng.*, 2023, **11**, 13778–13786.
11 C. H. Lee, T. H. Yang, Y. W. Cheng and C. J. Lee, *Constr. Build. Mater.*, 2018, **178**, 59–71.
12 J. Wen, B. Xue, F. Xu, R. Sun and A. Pinkert, *Ind. Crops Prod.*, 2013, **42**, 332–343.
13 Y. Xu, S.-C. Sun, C. Zhang, C.-Y. Ma, J. Wen and T. Yuan, *SSRN Electron. J.*, 2022, **462**, 142213.
14 C. Huang, G. Fang, Y. Zhou, X. Du, L. Yu, X. Meng, M. Li, C. G. Yoo, B. Chen, S. Zhai, Q. Guan, Q. Yong and A. J. Ragauskas, *ACS Sustainable Chem. Eng.*, 2020, **8**, 7380–7393.
15 Y. Zhan, J. Cheng, X. Liu, C. Huang, J. Wang, S. Han, G. Fang, X. Meng and A. J. Ragauskas, *Bioresour. Technol.*, 2022, **349**, 126854.
16 H. Zhang, X. Liu, S. Fu and Y. Chen, *Ind. Eng. Chem. Res.*, 2019, **58**, 13858–13867.
17 C. Huang, Y. Zhan, J. Wang, J. Cheng, X. Meng, L. Liang, F. Liang, Y. Deng, G. Fang and A. J. Ragauskas, *Green Chem.*, 2022, **24**, 3736–3749.
18 C. Huang, Y. Zhan, J. Cheng, J. Wang, X. Meng, X. Zhou, G. Fang and A. J. Ragauskas, *Bioresour. Technol.*, 2021, **326**, 124696.
19 M. A. Hossain, M. S. Rahaman, D. Yelle, H. Shang, Z. Sun, S. Renneckar, J. Dong, S. Tulaphol and N. Sathitsuksanoh, *Ind. Crops Prod.*, 2021, **167**, 113480.
20 Y. Liang, W. Duan, X. An, Y. Qiao, Y. Tian and H. Zhou, *Bioresour. Technol.*, 2020, **310**, 123389.
21 Y. H. Ci, F. Yu, C. X. Zhou, H. E. Mo, Z. Y. Li, Y. Q. Ma and L. H. Zang, *Green Chem.*, 2020, **22**, 8713–8720.
22 X. Shen, J. Wen, Q. Mei, X. Chen, D. Sun, T. Yuan and R. Sun, *Green Chem.*, 2019, **21**, 275–283.
23 Y. Wang, X. Meng, K. Jeong, S. Li, G. Leem, K. H. Kim, Y. Pu, A. J. Ragauskas and C. G. Yoo, *ACS Sustainable Chem. Eng.*, 2020, **8**, 12542–12553.
24 M. H. Tran, D. Phan and E. Y. Lee, *Green Chem.*, 2021, **23**, 4633–4646.
25 A. Zhang, X. Wu, X. Ouyang, H. Lou, D. Yang, Y. Qian and X. Qiu, *ACS Sustainable Chem. Eng.*, 2022, **10**, 9381–9388.
26 Y. Qian, Y. Deng, H. Li and X. Qiu, *Ind. Eng. Chem. Res.*, 2014, **53**, 10024–10028.
27 H. Zhang, F. Chen, X. Liu and S. Fu, *ACS Sustainable Chem. Eng.*, 2018, **6**, 12532–12540.
28 K. Biernacki, H. K. S. Souza, C. M. R. Almeida, A. L. Magalhães and M. P. Goncąlves, *ACS Sustainable Chem. Eng.*, 2020, **8**, 18712–18728.
29 Q. Liu, X. Zhao, D. Yu, H. Yu, Y. Zhang, Z. Xue and T. Mu, *Green Chem.*, 2019, **21**, 5291–5297.
30 S. D. Shinde, X. Meng, R. Kumar and A. J. Ragauskas, *Green Chem.*, 2018, **20**, 2192–2205.
31 Q. Xia, Y. Liu, J. Meng, W. Cheng, W. Chen, S. Liu, Y. Liu, J. Li and H. Yu, *Green Chem.*, 2018, **20**, 2711–2721.
32 J. Xie, J. Chen, Z. Cheng, S. Zhu and J. Xu, *Carbohydr. Polym.*, 2021, **269**, 118321.
33 N. Li, F. Meng, H. Yang, Z. Shi, P. Zhao and J. Yang, *Bioresour. Technol.*, 2022, **346**, 126639.
34 T. R. Mota, D. M. Oliveira, R. Simister, C. Whitehead, A. Lanot, D. Wanderley, C. A. Rezende, S. J. Mcqueen and L. D. Gomez, *Bioresour. Technol.*, 2021, **321**, 124499.
35 L. Zhao, Z. F. Sun, C. C. Zhang, J. Nan, N. Q. Ren, D. J. Lee and C. Chen, *Bioresour. Technol.*, 2022, **343**, 126123.
36 H. Ji and P. Lv, *Green Chem.*, 2020, **22**, 1378–1387.
37 S. Y. Jeong, B. Koo and J. W. Lee, *Ind. Crops Prod.*, 2022, **178**, 114569.
38 H. Zhang, Y. Bai, B. Yu, X. Liu and F. Chen, *Green Chem.*, 2017, **19**, 5152–5162.
39 Y. Liu, N. Deak, Z. Wang, P. J. Deuss, K. Barta, H. Yu, L. Hameleers and E. Jurak, *Nat. Commun.*, 2021, **12**, 5452.
40 X. Luo, Y. Li, N. K. Gupta, B. Sels, J. Ralph and L. Shuai, *Angew. Chem., Int. Ed.*, 2020, **59**, 11704–11716.
41 A. Tolbert, H. Akinosho and R. Khunsupat, *Biofuels, Bioprod. Biorefin.*, 2014, **8**, 836–856.
42 E. Capanema, M. Balakshin, R. Katahira, H. M. Chang and H. Jameel, *J. Wood Chem. Technol.*, 2014, **35**, 17–26.
43 M. T. Amiri, S. Bertella, Y. M. Questell-Santiago and J. S. Luterbacher, *Chem. Sci.*, 2019, **10**, 8135–8142.
44 F. Lu and J. Ralph, *J. Biobased Mater. Bioenergy*, 2011, **5**, 169–180.
45 M. Karlsson, J. Romson, T. Elder, Å. Emmer and M. Lawoko, *Biomacromolecules*, 2023, **24**, 2314–2326.
46 Y. Yu, W. Cheng, Y. Li, T. Wang, Q. Xia, Y. Liu and H. Yu, *Green Chem.*, 2022, **24**, 3257–3268.
47 O. Ajao, J. Jeaidi, M. Benali, A. M. Restrepo, N. El Mehdi and Y. Boumghar, *Molecules*, 2018, **23**, 377.
48 P. E. G. Loureiro, A. J. S. Fernandes, F. P. Furtado, M. G. V. S. Carvalho and D. V. Evtuguin, *J. Raman Spectrosc.*, 2011, **42**, 1039–1045.

49 C. S. Lancefield, I. Panovic, P. J. Deuss, K. Barta and N. J. Westwood, *Green Chem.*, 2017, **19**, 202–214.
50 Y. Qian, X. Qiu and S. Zhu, *Green Chem.*, 2015, **17**, 320–324.
51 J. Cheng, C. Huang, Y. Zhan, S. Han, J. Wang, X. Meng, C. Geun Yoo, G. Fang and A. J. Ragauskas, *Chem. Eng. J.*, 2022, **443**, 136395.
52 A. R. Mankar, A. Pandey and K. K. Pant, *Bioresour. Technol.*, 2022, **345**, 126528.
53 A. Pandey, R. Rai, M. Pal and S. Pandey, *Green Chem.*, 2014, **16**, 1559–1568.
54 S. C. Lee, E. Yoo, S. H. Lee and K. Won, *Polymers*, 2020, **12**, 699.
55 X. Meng, C. Crestini, H. Ben, N. Hao, Y. Pu, A. J. Ragauskas and D. S. Argyropoulos, *Nat. Protoc.*, 2019, **14**, 2627–2647.
56 B. Tang, K. Chong, A. J. Ragauskas and R. Evans, *ChemSusChem*, 2023, **16**, 1–8.
57 A. Sluiter, B. Hames, R. Ruiz, C. Scarlata, J. Sluiter, D. Templeton and D. Crocker, *Lab. Anal. Proced.*, 2008, 17.